Audio Engineering Society

Convention Paper

Presented at the 137th Convention
2014 October 9–12 Los Angeles, USA

Multiphysical Simulation Methods for Loudspeakers - Advanced CAE-based Simulations of Motor Systems

Alfred J. Svobodnik[1], Roger Shively[2], and Marc-Olivier Chauveau[3]

[1] Konzept-X GmbH, Karlsruhe, 76228, Germany
alfred.svobodnik@konzept-x.com

[2] JJR Acoustics, LLC, Seattle, Washington, 98467, USA
rshively@jjracoustics.com

[3] Moca Audio, Tours, 37100, France
mochauveau@moca-audio.com

ABSTRACT

This is the first in a series of papers on the details of loudspeaker design using multiphysical computer aided engineering simulation methods. In this paper, the simulation methodology for accurately modeling the electromagnetics of loudspeakers will be presented. Primarily, the creation of a useful impedance curve in the virtual world will be demonstrated. The influences of the mechanical mounting will also be illustrated, as well as the inherent non-linearities of the loudspeaker motor. Those non-linearities will be illustrated through the correct simulation of the electromagnetic driving force, which has an influence on all loudspeakers, and the voice coil inductance, which can have a profound influence on midrange and high frequency loudspeakers. Results will be presented, correlating the simulated model results to the measured physical parameters and to the impedance curve. From that, the important aspects of the modeling which determine its accuracy will be discussed.

1. INTRODUCTION

While typically the motor system of a loudspeaker can be treated as an axisymmetric device, and thus simplified 2D models can be applied for a majority of applications, its strong coupling to the structural domain (the loudspeaker's vibration system) via the voice coil acting in the magnet's air gap must be accounted for. For some motor structures also the variation of the flux field in axial direction is of crucial importance. Thus, typically finite element models for detailed motor design and optimization are being used.

At large excursions of the voice coil (when the loudspeaker is driven in the region of nominal power), a significant portion of the voice coil moves out of the main flux field, and thus less mechanical force is being induced. This nonlinear effect is very essential and causes unwanted distortion in the radiated sound. Additionally, voice coil inductance is also dependent on voice coil excursion and also on current. This leads to the need of nonlinear models to predict the loudspeaker behavior at large signals.

For system or subsystem level simulations (without the goal of designing a motor) 1D lumped models (additionally including nonlinearities to predict large signal behavior) are highly efficient. A lumped parameter model can be found in [1].

2. THEORY

2.1. Mathematical Background

The loudspeaker is driven by a time-harmonic voltage, $V = V_0\exp(i\omega t)$, applied to the voice coil. The following mathematical background section first describes the electromagnetic analysis of the current in the voice coil and the driving force that this current generates. [2] Once the relation between the driving voltage and the force is set up, the force is applied in a structure interaction analysis to finally compute the impedance curve.

As we are primarily focusing on electromagnetics, structure interaction is defined by linear lumped elements based on moving mass m_{ms}, compliance C_{ms} and mechanical damping Q_{ms}.

The Lorentz force on a wire of length L and with the current **I** in an externally generated magnetic flux density **B** perpendicular to the wire is given by $F = L\mathbf{I}\times\mathbf{B}$. The voice coil consists of a single copper wire making N_0 turns. The coil is considered to be homogeneous so that

$$N_0 I = \int_A J_\phi dA \quad (1)$$

where J_ϕ is the azimuthally directed current density through a cross-section of the coil, and the integral is taken over its area in the rz-plane (radial coordinates). The total driving force on the coil then becomes

$$F\mathrm{e} = -\int_V J\varphi B_r dV \quad (2)$$

with Br being the r-component of the magnetic flux density, and the integral evaluated over the volume occupied by the coil domain.

The current through the voice coil relates to the applied voltage as

$$I = V_0 + V_{be}/ Z_b \quad (3)$$

where Z_b is the blocked electric impedance and $-V_{be}$ denotes the back EMF.

To evaluate the back EMF, consider the same wire of length L in the magnetic flux density **B**, but now traveling at a velocity **v**. The wire gets an induced back EMF equal to $L\mathbf{v} \times \mathbf{B}$. The total back EMF in the coil equals to

$$-V_{be} = -v\frac{2\pi N_0}{A}\int \mathrm{rB}_r \mathrm{dA} \quad (4)$$

2.1.1. Static Solution

The first model solves for a static solution of the magnetic circuit in the loudspeaker motor structure. The iron in the pole piece and top plate is modeled as a nonlinear magnetic material, with the relation between the B and H fields coming from measured data. The static solution provides the magnetic field density at any point in the model. And, it provides the local effective relative permeability,

$$\mu_r = B/(\mu_0 H). \quad (5)$$

To calculate the force factor (BL) versus coil excursion (x) and Inductance (L_e) vs. x, there is a simplification performed. A moving mesh for the voice coil is used to obtain a static solution for each voice coil position in excursion. The results are the nonlinear behavior of the coil in a nonlinear field. Thus dynamics are excluded, which is valid as large excursions only happen in the low frequency range.

2.1.2. Nonlinear Model from Linearization

Static Solution Expanded into Frequency Domain

The linearization discussed here is for the nonlinear material model used for dynamic calculations. These are the calculations used to derive the Impedance curve.

The numerical sub steps in this model have a stationary step followed by a frequency domain step, such that the stationary solution defines the linearization point for the subsequent frequency domain solution. This means that the magnetic field derives and uses a differential permeability inherited from the one computed by the stationary step.

For the frequency domain assumption to be strictly valid, the applied AC voltage must be so small that the resulting current creates a magnetic field which does not significantly alter this permeability. Even though this is not quite the situation here, linearizing around a local biased permeability should still be a better approximation than assuming a constant permeability. The most accurate way to compute the impedance would be in a fully transient analysis, which is outside the scope of this paper.

In computing the structural interaction, the total voltage $V_0 + V_{be}$ and the resulting body load $-J_\phi B_r$ are applied to the coil domain being part of the structural domain.

The structural interaction is solved for only in the frequency domain sub step. The body load on the voice coil is entered as a product of the variables for the r-component of the magnetic flux density and the ϕ-component of the current density from the magnetic field. It is important to note that while the current density is time-harmonic, the magnetic flux density has both a static part caused by the permanent magnet and a time-harmonic part created by the coil itself. Only the external, static magnetic field should participate in the body load. The frequency domain solution should only consider contributions that are linear in the frequency.

3. SIMULATION MODEL

3.1. Model Setup

Setting up a model with all major AC/DC Computer Aided Engineering (CAE) software packages is straight forward and relatively simple. Starting point is a 2D cross section of the motor system as given in the following figure:

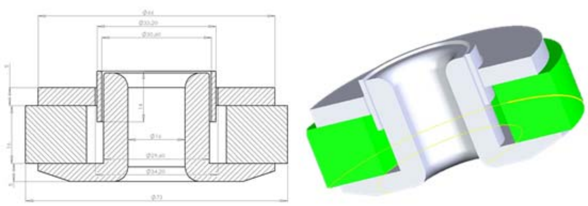

Figure 1. Geometry from CAD into Simulation

For more details on general CAE modeling, such as material definition, input parameters, applying physical laws, and parametric studies, we refer you to such references as [3].

3.2. Solutions

3.2.1. B Field

Figure 2 shows the magnetic field norm through the axisymmetric model. And Figure 3 shows the *BL* vs. *x*, derived from calculating BL in the moving mesh for the coil at each excursion point.

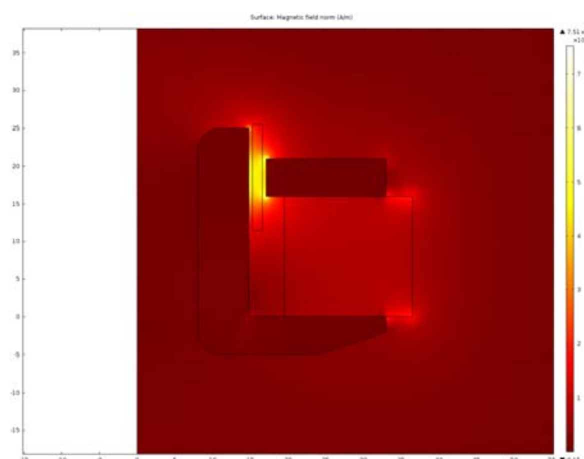

Figure 2. Magnetic Field Norm

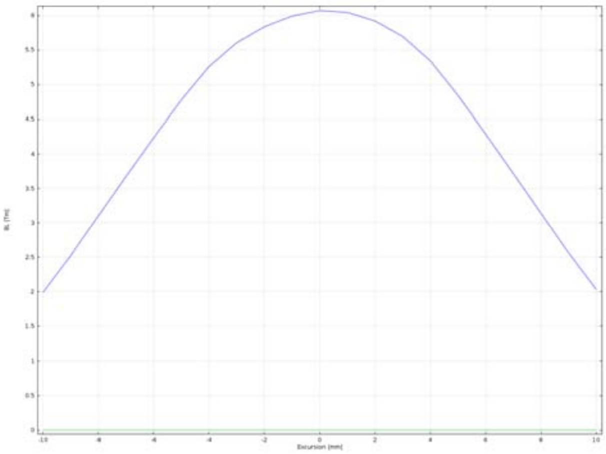

Figure 3. *BL* vs. *x*, calculated from moving mesh

3.2.2. Electromagnetic Permeability

Figure 4 shows the local effective relative permeability μ_r. The plot shows that the iron is close to saturation in the center of the pole piece, but remains in the linear realm above and below the magnet. This indicates that if you want to use less material, you can likely decrease the radius of the pole piece and top plate with very little effect on the magnetic field in the gap.

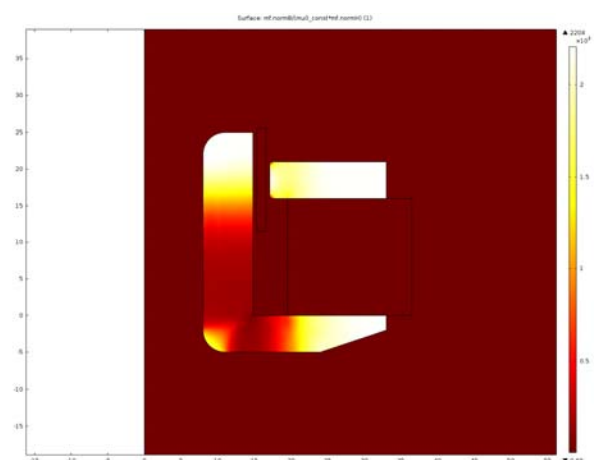

Figure 4. Local effective relative permeability $\mu_r = B/(\mu_0 H)$.

3.2.3. Induced Current Density (skinning Effect)

At the higher frequency, the skin effect brings the currents closer to the surfaces. This causes the inductance as well as the resistive part of the impedance to change with the frequency. Figure 5 shows the standard mesh, and Figure 6 the more refined mesh that accounts for the induced current density, shown in Figure 7 (Skin depths in practice will be tenths of millimeters, and a mesh element size of 0.2mm can be sufficient along the pole. Higher frequencies require smaller elements.) Figures 8 & 9 show the induced current at 1kHz and 10kHz, which we can relate to the blocked coil results after this in §3.2.4.

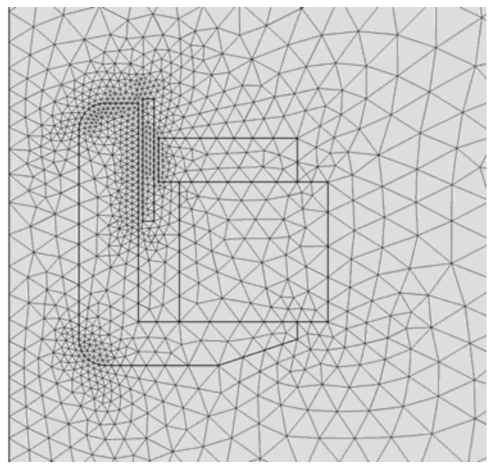

Figure 5. Standard Mesh

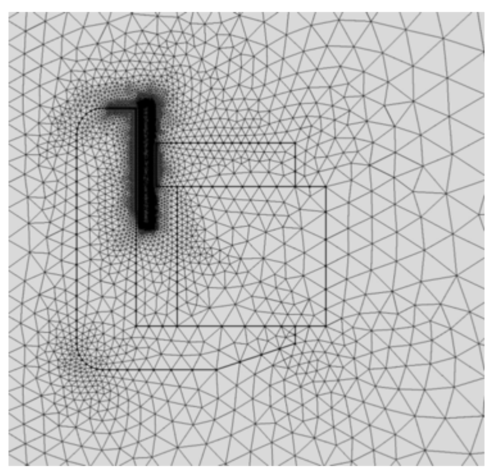

Figure 6. Refined mesh accounting for induced current density

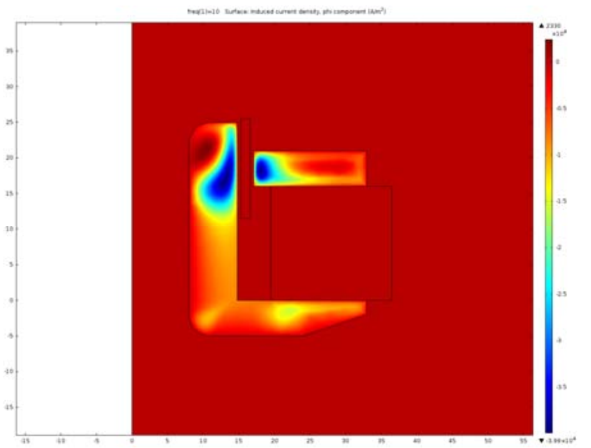

Figure 7. Induced Current Density (Skinning Effect).

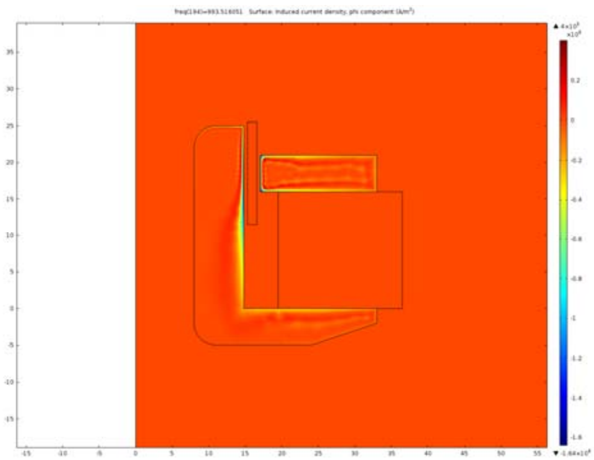

Figure 8. Induced Current Density @ 1kHz.

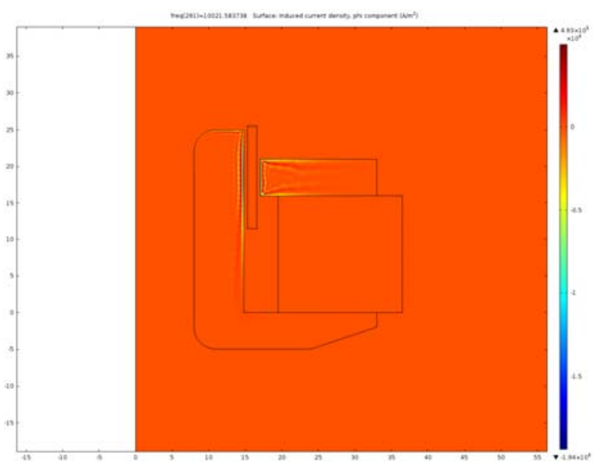

Figure 9. Induced Current Density @ 10kHz.

3.2.4. Blocked Coil Inductance (vs. Frequency)

In computing the blocked coil impedance, the AC equation is simplified by calculating a linear value around the local permeability resulting from the static solution. This is a straight forward small signal calculation. Figure 10 shows the induced currents versus frequency

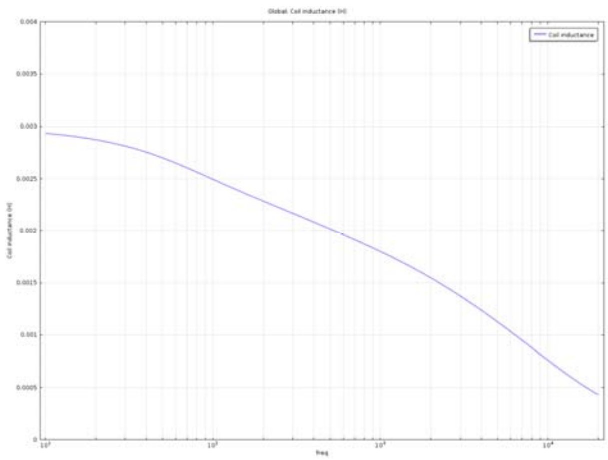

Figure 10. Coil Inductance vs. Frequency.

3.2.5. Variation of Blocked Inductance vs Excursion

Figure 11 shows the induced currents versus excursion, and Figure 12 shows the inductance as the coil moves in and out of the gap. Both are derived from the moving mesh for the coil.

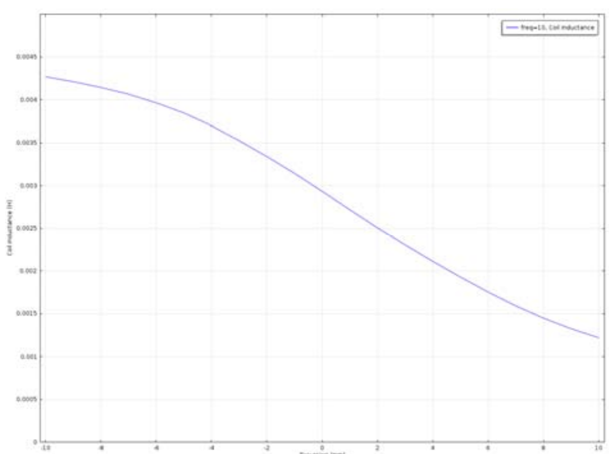

Figure 11. Electrical Inductance vs Coil Excursion

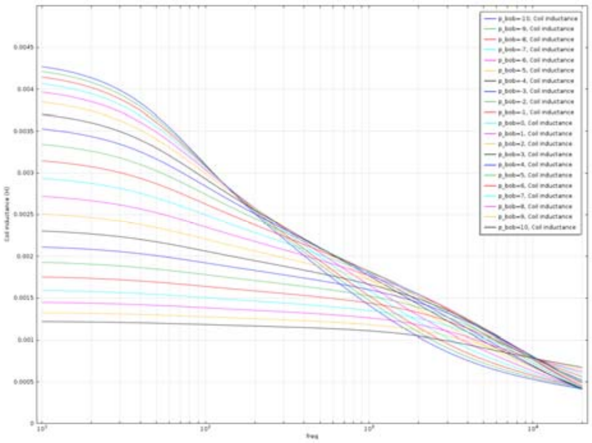

Figure 12. Derived Coil Inductance as the coil moves in and out of the gap

3.2.6. Total Electrical Impedance

The total electric impedance, defined as

$$Z = V_0/I, \tag{6}$$

appears in Figure 13. The peak at approximately 35 Hz coincides with the mechanical eigenfrequency - at this frequency the reactive part of the impedance switches from inductive to capacitive. In most of the operational range the impedance is largely resistive. At frequencies higher than 1 kHz, the impedance continues to increase as the inductance of the voice coil starts playing a more important part.

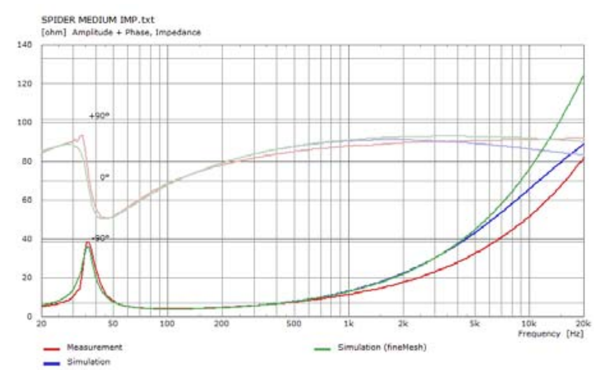

Figure 13. Total Electrical Impedance. (Measured vs. Simulated)

Here in Figure 13, the Red curve is measured data, the Blue curve is simulated data, and Green curve is the simulated data from a refined mesh (as discussed in §3.2.3).

3.2.7. Force "Body Load"

As mentioned there is a strong coupling of the loudspeaker motor to the structural domain of the loudspeaker's vibration system through the voice coil. Figure 14 illustrates the voice coil force (body load) that is transferred directly. There are additional body loads applied to the components of the motor structure itself, which could also be transferred to additional structural members (i.e., mounting brackets and frames for the loudspeaker). Figures 15 & 16 illustrate the body loads concentrated on the motor front plate at 100Hz and 1kHz. The extent of these body forces will be part of future discussions, which are outside the scope of this paper.

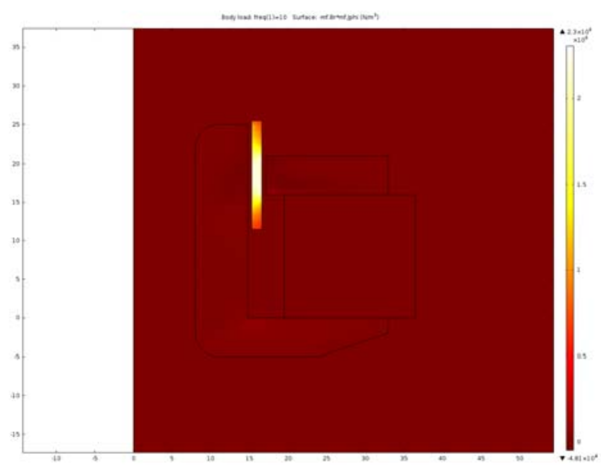

Figure 14 Voice Coil Force (body load)

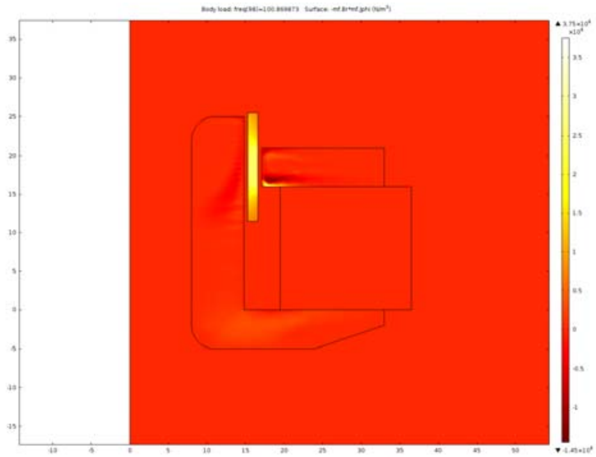

Figure 15. Body loads at 100Hz

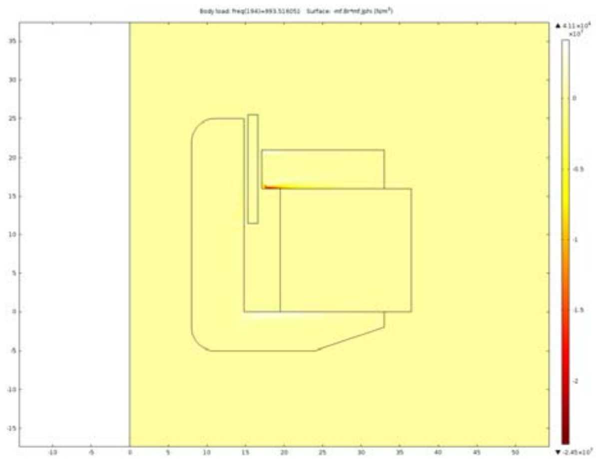

Figure 16. Body loads at 1kHz

4. MEASUREMENTS

The motor structure used in the simulation and defined by the CAD data is a ∅73mm ferrite magnet motor for a ∅33mm voice coil used in a subwoofer design. It was a 3.4 Ω DCR coil, with ∅0.31mm copper wire, which was wound into a 14mm long two-layer coil.

Measurements were done using sweep sinusoid input at a low level, with the loudspeaker in free air. The resolution of the measurement data was 1/24 octave. A two-channel impedance measurement is completed. This is the red curve in Figure 13. Thiele-Small parameters were calculated using the added mass technique, and least square error curve fit, to determine the comparison values for the static force factor (*BL*) and for the Inductance (L_e) at 1kHz and 10kHz.

$BL = 6.1005$ T·m

$L_e = 1.4$mH @1kHz and 0.72mH @10kHz

5. FINAL COMMENTS

When we look in detail at the impedance curves from measurements and refined simulation, we can identify differences in high frequency impedance, but not in inductance (@10kHz). This presents an excellent opportunity for future exploration of the true nature of loudspeaker voice coil current in electromagnetic fields.

The potential for properly defining the voice coil impedance and inductance behavior and its effect on the loudspeaker's frequency response, is greater with these CAE simulation methods than using empirical, predictive solutions of the recent past [4, 5, 6].

The audio industry, as well as most industries today, is challenged by the need to (constantly) increase engineering efficiency. CAE based on simulation and analysis of the functional performance of products plays already a key role for more than two decades. CAE methodologies are today typically used at every stage of the development cycle, from first concept studies up to detailed engineering for final product development to be released to the market place (including modeling of the manufacturing processes as well). During the last years a strong trend for moving CAE upfront in the design process (to be applied already in the concept phase) can be monitored. Thus the term frontloaded Virtual Product Development (VPD) is often used. The advantages for moving CAE upfront are:

- more freedom in the design decisions
- design changes can be made at lower costs

These advantages additionally fulfill the above mentioned basic requirements to increase engineering efficiency. Similar thoughts have been applied to the automotive industry [7].

This frontloaded approach was first (successfully) introduced for the development of automotive and aerospace key components at the OEMs. A good example for a first application of VPD is the development of car body structures with respect to crashworthiness, fatigue or NVH behavior. Today it is stringent for almost all industries to follow the path of a frontloaded VPD cycle as well.[1]

As for the topic of this paper, we can precisely see that advanced CAE methods can accurately predict the functional performance of motor systems. Thus we can optimize designs in a very early design stage where no physical prototypes exist. Here again, CAE methods are key technologies to optimize product development in terms of performance and cost, resulting in optimization of engineering efficiency in general.

6. REFERENCES

[1] A. J. Svobodnik, "Multiphysical Simulation Methods for Loudspeakers - A (Never-)Ending Story?", 136th AES Convention, 2014

[2] J. A. Stratton, *Electromagnetic Theory*, (John Wiley & Sons, New Jersey, 2007; reprinted from original edition 1941)

[3] COMSOL Multiphysics 4.4., Model Library, © 1998-2013 COMSOL AB

[4] W. M. Leach, Jr., "Loudspeaker Voice Coil Inductance Losses", J. Audio Eng. Soc, Vol. 50, No. 6, pp 442-450 (2002 June).

[5] M. Dodd, "The Transient Magnetic Behaviour of Loudspeaker Motors", 111th AES Convention, 2001.

[6] G. Pillonnet et al, "Distortion Improvement in the Current Coil of Loudspeakers", 134th AES Convention, 2013.

[7] AUTOSIM Consortium, "Current & Future Technologies in Automotive Engineering Simulation", NAFEMS, 2008